

Collective Effects of Organic Molecules based on Holstein-Tavis-Cummings Model

Quansheng Zhang¹ and Ke Zhang^{2,3}

¹*Beijing Computational Science Research Center, Beijing 100193, China**

²*Helmholtz Institute Mainz, GSI Helmholtzzentrum für Schwerionenforschung, 55099 Mainz, Germany*

³*Johannes Gutenberg-University Mainz, 55099 Mainz, Germany*

(Dated: December 4, 2021)

We study the collective effects of an ensemble of organic molecules confined in an optical cavity based on Holstein-Tavis-Cummings model. By using the quantum Langevin approach and adiabatically eliminating the degree of freedom of the vibrational motion, we analytically obtain the expression of the cavity transmission spectrum to analyze the features of polaritonic states. As an application, we show that the dependence for the frequency shift of the lower polaritonic state on the number of molecules can be used in the detection of the ultra-cold molecules. We also numerically analyze the fluorescence spectrum. The variation of the spectral profile with various numbers of molecules gives signatures for the modification of molecular conformation.

I. INTRODUCTION

The interaction between molecule and light has played an important role in photochemical reactivity [1], molecular spectroscopy [2, 3], chemical fingerprinting [4], and the generation of non-classical states of light [5]. When molecules located in an optical cavity, the coupling strength can be enhanced [6–9]. In the strong coupling regime, the energy may oscillate between molecules and cavity field at a faster rate than their relaxation rates, inducing that the molecular and photonic states are hybridized into polaritonic states [10]. In this situation, the potential energy landscape for the molecular conformation will be modified, giving rise to a range of further effects on the material properties of the molecules. As the modifications for molecular conformation are tunable, it has opened up new routes for the control of chemical reactivity [11, 12], energy and charge transport [13, 14], and Förster resonance energy transfer [15–17]. Besides, the modifications for molecular conformation will bring influence on the profile of molecular absorption and fluorescence spectra [18]. For the electronic transitions, the coupling between electronic state and the molecular conformation will lead to the structure of the emission (or absorption) spectra observed in experiments [9, 19] with multiple peaks. The observable molecular spectra will give signatures for the variation of molecular conformation.

To provide an understanding of such phenomena, the Holstein-Tavis-Cummings (HTC) model has been widely adopted to describe the light-electronic-vibration problem [18, 20]. Furthermore, an approach based on the quantum Langevin equation to solve the HTC model has been developed recently [17]. It provides an alternative path to understand the Stokes and anti-Stokes processes [17], Purcell effect under the influence of the phononic environments [21], and the Floquet engineering [22] at the level of operators rather than states. However, the previous works [17, 21, 22] mainly focus on a single molecule. When multiple molecules confined in a cavity, the system will experience more complex dynamics. In the case that many molecules are intro-

duced to couple a quantized cavity field, an efficient interaction between molecules will be induced, leading to collective effects [23]. On the other hand, the description of the electronic transition dressed by the vibrational motion suggests that the vibrators for one molecule will be coupled to that for other molecules. Considering above facts, a profound influence will be brought on the polaritonic states, as well as the fluorescence (or absorption) spectrum.

Inspired of this, we provide here a further study of HTC model when multiple molecules are presented. Going from a set of coupled standard Langevin equations for the whole system, and adiabatically eliminating the degree of freedom of the vibrational motion, a set of effective equations can be derived, involving the average values of Pauli operators, photonic operators and their correlations. From these equations, we study the collective effects in the optical cavity via the cavity transmission spectrum, the steady population and the fluorescence spectrum. To test the reasonableness of approximation, we perform a numerical simulation for the case of two molecules in the limit of weak coupling between the electronic states and molecular conformation with help of the QuTiP package [24], and also take perturbative treatment in the first order to compare against the perturbative method in second order for general situations. We show that the profiles of cavity transmission spectrum and the fluorescence spectrum can be modified via the number of molecules, which will give signatures of the modification of molecular conformation. Such phenomena will provide potential applications in the detection of untracold molecules [25], as well as the control of chemical reaction [12, 26], energy and charge transport [14, 20], and so on. In contrast, we also give the analysis of a special case in the limit of without the coupling between electronic states and molecular conformation, i.e. Tavis-Cummings (TC) model.

The structure of this paper is organized as following. In Sec. II, we describe the model and give the formal solution about the average value of the Pauli lowering operator with the adiabatic elimination for the degree of freedom vibrational motion. In Sec. III, we investigate the influence of the number of molecules on the polaritonic features via the cavity transmitted field for HTC model and TC model, respectively. In Sec. IV, we analyze the influence of the number of molecules on the fluorescence spectrum for HTC model and TC model,

* qshzhang@csrc.ac.cn

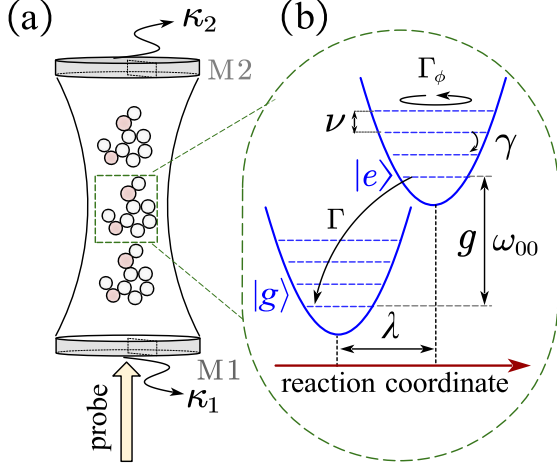


Figure 1. (Color online) Model schematics. (a) An ensemble of N organic molecules are placed inside a Fabry-Pérot microcavity with a single mode. The dissipation for the cavity field occurs at rates κ_1 through the mirror M1 and κ_2 through the mirror M2. (b) Diagram of molecular level structure and relaxation processes. Each molecule is represented by two harmonic oscillator potential surfaces of two electronic states with the shift λ in reaction coordinate. The cavity field resonantly couples to the electronic transition $|g\rangle \leftrightarrow |e\rangle$ with the coupling strength g . The relaxation processes of each molecule include the electronic decay at rate Γ , and the pure dephasing at rate Γ_ϕ and internal vibrational relaxation at rate γ .

respectively. Finally, a summary is given in Sec. V.

II. MODEL

As illustrated in Fig. 1, the proposed system of interest consists of an ensemble of N organic molecules, which are confined in a Fabry-Pérot microcavity. Considering the organic molecules comprised of z atoms, there will be $3z-6$ (or $3z-5$ for linear molecules) normal modes of vibration in the configuration space of the nuclear coordinates [11, 20]. When describing a chemical reaction, often a few of these modes, which are associated with the reaction coordinates, are investigated [11, 20, 27]. For a single reaction coordinate, one can assume that the vibrational frequencies for the ground and excited electronic states are the same. Thus, the system can be represented as a two-level system (corresponding to its ground $|g_m\rangle$ and excited $|e_m\rangle$ electronic states) and a phonon mode (denoting the harmonic vibrational degree of freedom with the annihilation operator b_m). Here, each molecule is labeled by the index m (running from 1 to N). The dynamic for a single free molecule is then governed by the Holstein Hamiltonian [20]

$$H_m = \nu b_m^\dagger b_m + [\omega_e + \lambda\nu(b_m + b_m^\dagger)]\sigma_m^\dagger \sigma_m, \quad (1)$$

where $\omega_e = \omega_{00} + \lambda^2\nu$ is the effective transition frequency, with ω_{00} being the bare splitting between the ground and excited electronic states, and ν is the vibrational frequency for

the harmonic oscillator. The parameter λ is related with the Huang-Rhys factor S , i.e. $S = \lambda^2$. Here S ranges from 0 to ~ 2 [28–30], resulting from the displacement of the equilibrium position of the vibrational mode between the excited and ground electronic states. Furthermore, λ also characterizes the coupling between the electronic states and molecular conformation. In the limit of $\lambda = 0$, one can simplify the system for the molecule described by Eq. (1) to be a two-level system.

When the cavity field is single-mode, the molecule-cavity interaction can be depicted by the TC Hamiltonian (we set $\hbar = 1$)

$$H_{\text{int}} = \omega_c a^\dagger a + g \sum_{m=1}^N (a^\dagger \sigma_m + \text{H.c.}), \quad (2)$$

where the operator a annihilates a cavity photon at frequency ω_c , $\sigma_m = |g_m\rangle\langle e_m|$ annihilates the molecular excitation and g is the coupling strength for a single molecule. Notably, this Hamiltonian implies the assumption that all molecules are equally coupled to the cavity field via neglecting the influences resulting from the disorder of transition dipole moment of molecules and molecular spatial distribution. Such approximation will conveniently provide a qualitative description of the collective behavior for organic polaritons [31].

Taking account of the free part of the molecules and the situation that the cavity is probed by a classical field at frequency ω_l with the coupling strength η , the total Hamiltonian for such system in the rotating wave approximation can be given

$$H = \sum_m H_m + H_{\text{int}} + i\eta(ae^{i\omega_l t} - a^\dagger e^{-i\omega_l t}). \quad (3)$$

Applying a polaron transformation $H_p = U^\dagger H U$ with

$$U = \exp\left[\sum_m \lambda \sigma_m^\dagger \sigma_m (b_m - b_m^\dagger)\right], \quad (4)$$

one can recast the Hamiltonian (3) into

$$H_p = \sum_m (\nu b_m^\dagger b_m + \omega_{00} \sigma_m^\dagger \sigma_m) + \omega_c a^\dagger a + \left(\sum_m g \mathcal{D}_m^\dagger \sigma_m a^\dagger + i\eta e^{i\omega_l t} a + \text{H.c.}\right), \quad (5)$$

where $\mathcal{D}_m = \exp[\lambda(b_m - b_m^\dagger)]$ is a displaced operator for m -th molecule. In this representation, the coupling between the two-level system and cavity field is dressed by vibrations via the Frank-Condon factors ${}_{\text{vib}}\langle n | \mathcal{D} | m \rangle_{\text{vib}}$ for the transition $|g\rangle |n\rangle_{\text{vib}} \rightarrow |e\rangle |m\rangle_{\text{vib}}$, where $|n\rangle_{\text{vib}}$ (or $|m\rangle_{\text{vib}}$) are Fock states for vibrations.

To model the open system, we should consider the relaxation processes as depicted in Fig. 1(b), including the loss of cavity field at rate $\kappa = \kappa_1 + \kappa_2$ (encompassing losses via both mirrors), the spontaneous emission of the electronic transition

at rate Γ , and the pure dephasing of the electronic transition at rate Γ_ϕ . Their effects are described as Lindblad terms, and represented by $\mathcal{L}_{\gamma_O}[\mathcal{O}] = \gamma_O(2\mathcal{O}\rho\mathcal{O}^\dagger - \mathcal{O}^\dagger\mathcal{O}\rho - \rho\mathcal{O}^\dagger\mathcal{O})$ with a collapse operator \mathcal{O} and a corresponding decay rate γ_O . Finally the dynamics of the system can be described by a master equation of the density matrix ρ

$$\begin{aligned} \dot{\rho} = & -i[H, \rho] + \mathcal{L}_\kappa[a] + \sum_m^N \mathcal{L}_{\Gamma_\phi}[\sigma_m^\dagger\sigma_m - \sigma_m\sigma_m^\dagger] \\ & + \sum_m^N \mathcal{L}_\Gamma[\sigma_m] + \sum_m^N \mathcal{L}_\gamma[b_m]. \end{aligned} \quad (6)$$

The last term in Eq. (6) represents the vibrational relaxation process at rate γ . Physically, when considering the coupling between the vibrator and a reservoir of phonons (also described as Brownian noise dissipation model [17, 21]) in a solvent or surrounding medium, the vibrational relaxation of molecules cannot be simply expressed in Lindblad form [21, 22, 32]. In this work, for the sake of convenience to discuss, we still adopt the Lindblad decay model to describe the vibrational relaxation process. This approach has been used in several theoretical studies to explore the molecular spectroscopy [17, 22], Purcell effect [21], energy transfer [17] and organic polariton lasing [33]. In the limit $\lambda^2\gamma \ll \Gamma$, the Lindblad decay model for the vibrational relaxation will be indistinguishable to the Brownian noise model [17, 22]. Additionally, the spontaneous emission is also involved in the vibrational motion, which can be ignorable due to its decay rate much smaller than the vibrational relaxation rate γ .

The master equation method is usually equivalent to the Langevin approach. For the given master equation in the Lindblad form, described as $\mathcal{L}_{\gamma_O}[\mathcal{O}]$ with a collapse operator \mathcal{O} and decay rate γ_O , we can map it onto a Langevin form [34]

as

$$\begin{aligned} \frac{d}{dt}\mathcal{A} = & i[H, \mathcal{A}] - \sum_j \left[\mathcal{A}, \mathcal{O}_j^\dagger \right] \left\{ \gamma_{\mathcal{O}_j} \mathcal{O}_j - \sqrt{2\gamma_{\mathcal{O}_j}} \mathcal{O}_j^{\text{in}} \right\} \\ & + \sum_j \left\{ \gamma_{\mathcal{O}_j} \mathcal{O}_j^\dagger - \sqrt{2\gamma_{\mathcal{O}_j}} \mathcal{O}_j^{\text{in}\dagger} \right\} [\mathcal{A}, \mathcal{O}_j], \end{aligned} \quad (7)$$

with an arbitrary system operator \mathcal{A} and any collapse operator \mathcal{O}_j in the set $\{b_m, \sigma_m, \sigma_m^\dagger\sigma_m - \sigma_m\sigma_m^\dagger, a\}$.

Under the condition of weak driving $\eta \ll \kappa$, the cavity field in steady situation will have much less one photon and the molecules will pretty much stay in the electronic ground state, i.e. $\sigma_m^\dagger\sigma_m \ll 1$. In the rotating frame at the probe frequency ω_l , the quantum Langevin equations for the cavity field a , and polarized operator $\tilde{\sigma}_m = \mathcal{D}_m^\dagger\sigma_m$ are given as [17]

$$\begin{aligned} \frac{d}{dt}a = & -(i\Delta_c + \kappa)a - ig \sum_m^N \sigma_m + \sqrt{2\kappa_1}A_{\text{in}} \\ & + \sqrt{2\kappa_2}a_2^{\text{in}}(t), \end{aligned} \quad (8a)$$

$$\frac{d}{dt}\tilde{\sigma}_m \approx -(i\Delta + \Gamma_\perp)\tilde{\sigma}_m - ig\mathcal{D}_m^\dagger a + \sqrt{2\Gamma_\perp}\mathcal{D}_m^\dagger\sigma_m^{\text{in}}, \quad (8b)$$

with the detuning $\Delta_c = \omega_c - \omega_l$ and $\Delta = \omega_{00} - \omega_l$. Here, $\Gamma_\perp = \Gamma + 2\Gamma_\phi$ is the effective transverse relaxation rate. Notably, under the description of the vibrational relaxation in the Lindblad form, an additional dephasing will be caused to the polarized operator. However, we can neglect such dephasing as this will lead to the disagreement with experimental observations of lifetime for the electronic transition [17, 21, 22]. Additionally, $A_{\text{in}}(t) = \eta/\sqrt{2\kappa_1} + a_1^{\text{in}}(t)$ denotes the effective cavity input with zero-average input noise $a_1^{\text{in}}(t)$. Here we assume that the temperature for cavity field is zero, i.e. $T_{\text{cav}} = 0$, then the non-vanishing correlation $\langle a_1^{\text{in}}(t)a_1^{\text{in}\dagger}(t') \rangle = \delta(t - t')$ and $\langle a_2^{\text{in}}(t)a_2^{\text{in}\dagger}(t') \rangle = \delta(t - t')$ will be obtained. The electronic transition is also affected by a white noise input σ_m^{in} with nonzero correlation $\langle \sigma_m^{\text{in}}(t)\sigma_n^{\text{in}\dagger}(t') \rangle = \delta_{mn}\delta(t - t')$.

Then we can formally integrate the Eq. (8b) to get the solution for $\tilde{\sigma}_m$ and subsequently for Pauli lowering operator

$$\sigma_m(t) = - \int_0^t dt_1 e^{-(i\Delta + \Gamma_\perp)(t-t_1)} \mathcal{D}_m(t) \mathcal{D}_m^\dagger(t_1) [iga(t_1) - \sqrt{2\Gamma_\perp}\sigma_m^{\text{in}}(t_1)] + e^{-(i\Delta + \Gamma_\perp)t} \mathcal{D}_m(t) \mathcal{D}_m^\dagger(0) \sigma_m(0). \quad (9)$$

In a solvent or surrounding medium, the coupling between the vibrator and a reservoir of phonons will lead to large relaxation rate for vibrational motion (i.e., $\gamma \gg \Gamma_\perp$) [21, 32, 35]. Additionally, we also assume that the vibrational relaxation rate much larger than cavity field (i.e., $\gamma \gg \kappa$). Under these conditions, the timescale of vibrational relaxation will be much shorter than that for the relaxation of electronic state, and also the decay of cavity field. Therefore, the vibrational

state may be considered to be in the steady state [32]. Via treating the vibrations as a Markovian phonon bath [32, 36], the degrees of freedom for cavity field and vibrational motion can be separated as

$$\langle a(t_1) \mathcal{D}_m(t) \mathcal{D}_m^\dagger(t_1) \rangle \approx \langle a(t_1) \rangle \langle \mathcal{D}_m(t) \mathcal{D}_m^\dagger(t_1) \rangle, \quad (10)$$

as well as that for Pauli lowering operators and vibrational

motion

$$\langle \sigma_n(t_1) \mathcal{D}_m(t) \mathcal{D}_m^\dagger(t_1) \rangle \approx \langle \sigma_n(t_1) \rangle \langle \mathcal{D}_m(t) \mathcal{D}_m^\dagger(t_1) \rangle. \quad (11)$$

If these molecules are initially prepared in the ground electronic state, and zero photon populated in cavity, the last term in Eq. (9) will be canceled when we take average over the cavity field, the vibrational motion, and the electronic state. Finally, the average dipole moment $\langle \sigma_m \rangle$ can be derived

$$\langle \sigma_m \rangle = -ig \int_0^\infty dt_1 \mathcal{F}_m(t - t_1) \langle a(t_1) \rangle, \quad (12)$$

with the definition $\mathcal{F}_m(t - t_1) = \Theta(t - t_1) \exp[-(i\Delta + \Gamma_\perp)(t - t_1)] \langle \mathcal{D}_m(t) \mathcal{D}_m^\dagger(t_1) \rangle$, where $\Theta(t)$ is the Heaviside step function. The two-time correlation for the displacement operators $\langle \mathcal{D}_m(t) \mathcal{D}_m^\dagger(t_1) \rangle$ can be expressed as (at $t > t_1$)

$$\langle \mathcal{D}_m(t) \mathcal{D}_m^\dagger(t_1) \rangle = e^{-\lambda^2} e^{\lambda^2 e^{-(\gamma + i\nu)(t - t_1)}}, \quad (13)$$

when the effective vibrational temperature satisfies $k_B T_{\text{vib}} / \hbar \nu \ll 1$ (see Appendix A). The important quantity to be emphasized is the function $\langle \mathcal{D}_m(t) \mathcal{D}_m^\dagger(t_1) \rangle$, which implies the influence of the vibrational mode on the excitons in organic molecules. When $\lambda = 0$, one can achieve the value of the function $\langle \mathcal{D}_m(t) \mathcal{D}_m^\dagger(t_1) \rangle = 1$. Then the interaction between electronic states and molecular conformation will be removed. For finite λ , the coupling between the vibrational mode and the excitons will result in some new fascinating physics.

Notably, the Pauli operator can feed back into itself via the cavity field, resulting in higher order correlation between the displaced operators. The adiabatic approximation depicted by Eq. (13) has neglected the contributions from these higher order correlations. To explore the influence of these higher order correlations, we have taken further discussion in Appendix B and C.

III. CAVITY TRANSMISSION

For the molecule-cavity system discussed in the previous section, the electronic transition will be dressed by vibrational motion with the coupling between the electronic states and molecular conformation. In the limit of large vibrational relaxation (i.e. $\gamma \gg \kappa$ and $\gamma \gg \Gamma_\perp$), the vibrational mode can be treated as a locale phonon reservoir under the Markov approximation. Going from the Langevin equation of polarized operator and adiabatically eliminating the degree of freedom of vibrational motion, we formally derive the expression of the average Pauli lowering operator $\langle \sigma_m \rangle$. It is noteworthy that the first term in Eq. (12) represents a convolution. This character will inspire us to utilize the Laplace transformation (defined as $\langle \bar{f} \rangle(s) = \int_0^\infty dt f(t) e^{-st}$ for time dependent function $f(t)$ at $t \geq 0$) to simplify the derivation. Then, Eq. (12) can be reformed as

$$\langle \bar{\sigma}_m \rangle = -ig \bar{\mathcal{F}}_m(s) \langle \bar{a} \rangle, \quad (14)$$

where $\bar{\mathcal{F}}_m$ is the Laplace transform of $\mathcal{F}_m(t)$, expressed as

$$\bar{\mathcal{F}}_m = \sum_k \frac{\lambda^{2k}}{k!} \frac{e^{-\lambda^2}}{s + i(\Delta + k\nu) + (\Gamma_\perp + k\gamma)}, \quad (15)$$

with the Laplace transform variable s . Similarly, taking average over the cavity field as well as the electronic degrees of freedom on both sides of Eq. (8a), and applying the Laplace transformation, we finally obtain

$$s \langle \bar{a} \rangle = -(i\Delta_c + \kappa) \langle \bar{a} \rangle - ig \sum_m^N \langle \bar{\sigma}_m \rangle + \frac{\eta}{s}. \quad (16)$$

Considering the system with N identical molecules, the Laplace form for the average Pauli lowering operator $\langle \bar{\sigma}_m \rangle$ and the function $\bar{\mathcal{F}}_m(s)$ would be the same for any molecule (m). Combining the Laplace forms of the Pauli operator described by Eq. (14) and the cavity field illustrated by Eq. (16), we can get

$$\langle \bar{\sigma}_m \rangle = -\frac{ig\eta \bar{\mathcal{F}}_m}{s[Ng^2 \bar{\mathcal{F}}_m + i\Delta_c + \kappa + s]}, \quad (17a)$$

$$\langle \bar{a} \rangle = \frac{\eta}{s[i\Delta_c + s + \kappa + Ng^2 \bar{\mathcal{F}}_m]}. \quad (17b)$$

From the final value theorem [37], we get the steady values

$$\langle \sigma_m \rangle_{\text{ss}} = \lim_{s \rightarrow 0} s \langle \bar{\sigma}_m \rangle = -\frac{ig\eta\chi}{i\Delta_c + \kappa + Ng^2\chi}, \quad (18a)$$

$$\langle a \rangle_{\text{ss}} = \lim_{s \rightarrow 0} s \langle \bar{a} \rangle = \frac{\eta}{(i\Delta_c + \kappa) + Ng^2\chi}, \quad (18b)$$

where “ss” stands for the steady state situation, and $\chi = \lim_{s \rightarrow 0} \bar{\mathcal{F}}_m$. The item $Ng^2\chi$ in Eq. (18b) reflects the hybridization between photonic states and molecule electronic states. One can approximately obtain the hybridized decay rates and frequencies (under resonance conditions, i.e., fixed $\Delta = \Delta_c = 0$) [10, 38]

$$\Gamma_\pm = \frac{\Gamma_{\text{eff}} + \kappa}{2} \pm \Re \sqrt{\frac{(\Gamma_{\text{eff}} + i\Delta_{\text{eff}} - \kappa)^2}{4} - Ng^2}, \quad (19a)$$

$$\omega_\pm = -\frac{\Delta_{\text{eff}}}{2} \pm \Im \sqrt{\frac{(\Gamma_{\text{eff}} + i\Delta_{\text{eff}} - \kappa)^2}{4} - Ng^2}, \quad (19b)$$

where $\Gamma_{\text{eff}} = \Re \lim 1/\chi$ and $\Delta_{\text{eff}} = \Im \lim 1/\chi$ denote the effective decay rate and additional frequency shift for excitons, respectively.

In experiments, the hybridized decay rates and frequencies can be detected via the cavity transmitted field. According to the input and output relation $a_{2,\text{out}}(t) = \sqrt{2\kappa_2} a(t)$, the transmission \mathcal{T} via $\mathcal{T} = \langle a_{2,\text{out}} \rangle_{\text{ss}} / \langle A_{\text{in}} \rangle_{\text{ss}}$ in steady state reign will be expressed as

$$\mathcal{T} = \frac{2\sqrt{k_1 k_2}}{(i\Delta_c + \kappa) + Ng^2\chi}. \quad (20)$$

Figures 2(a-f) plot the intensity of the cavity transmission at resonance $\omega_c = \omega_{00}$ in the various number N of the

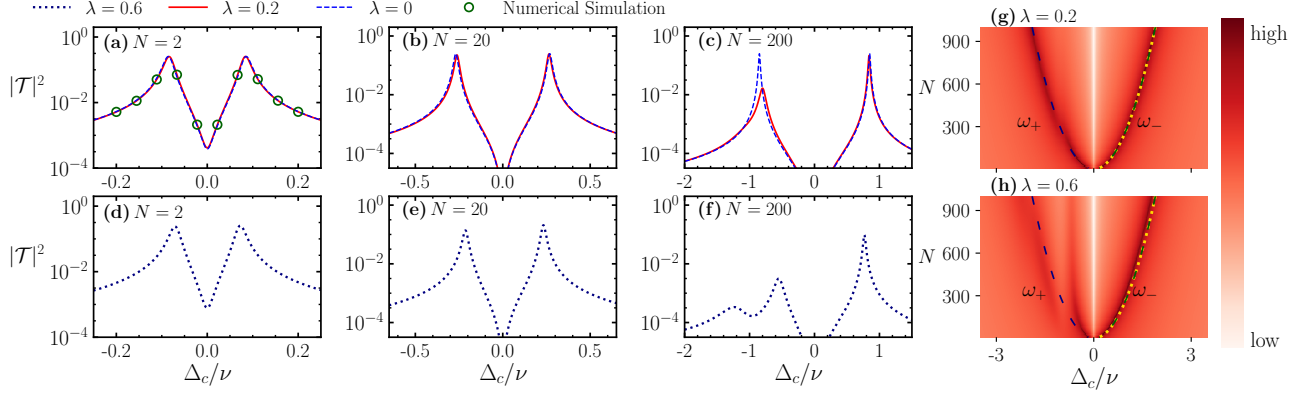


Figure 2. (Color online) Cavity-molecule spectroscopy. (a-f) Influence of the number N (increases as 2, 20, and 200) of identical organic molecules on the intensity of transmitted field at resonance $\omega_c = \omega_{00}$ at $\lambda = 0$ (blue dashed line), $\lambda = 0.2$ (red solid line) and $\lambda = 0.6$ (black dotted line), respectively. (a) The green circle marks shows the numerical simulation results for the case $\lambda = 0.2$, $N = 2$ with the help of QuTiP. Intensity of transmitted field at resonance $\omega_c = \omega_{00}$ as a function of the detuning Δ_c/ν and the number N of organic molecules at $\lambda = 0.2$ (g) and $\lambda = 0.6$ (h), respectively. The spatial intensity profile of the transmitted field is shown in arbitrary units but to scale. The green and blue dashed lines show the frequency shift of the lower and upper polaritonic states various the number N of organic molecules, respectively, given by Eq. (19b). The frequency shift of the lower polaritonic state is about $\omega_- \approx g\sqrt{N}$ (yellow dotted line). The other parameters are $\nu/\Gamma = 250$, $\Gamma_\phi/\Gamma = 2\kappa_1/\Gamma = 2\kappa_2/\Gamma = 1$, $\gamma/\Gamma = 50$, $g/\Gamma = 5$, and $\eta/\Gamma = 0.01$.

organic molecules for TC (see blue dashed line) and HTC (see red solid line and black dotted line) model, respectively. The parameters we chosen are given in the caption of Fig. 2, which associate with the recent theoretical researches [17, 21, 22, 33]. When multiple molecules emerged in a cavity, the system will be in the collective behavior with a bright mode that couples to the cavity field with an enhanced strength $g\sqrt{N}$ (for identical molecules). In the limit of $\lambda = 0$, [see blue dashed line in Fig. 2(a-c)], the cavity transmission will be split into two symmetric peaks with the central frequency separation $2\sqrt{N}g^2 - (\Gamma_\perp + \kappa)^2/4$ [38–40].

For finite λ , the coupling between electronic states and molecular conformation will produce additional dephasing as well as the frequency shift for excitons, resulting in an asymmetric cavity transmission profile [see red solid line in Fig. 2(c) and black dotted line in Figs. 2(d-f)]. In the limit of $\lambda^2 \ll 1$ and $g\sqrt{N} \ll \nu$, the evolution of the transmitted field for HTC model with the detuning Δ_c will perform similar behaviors to the TC model, due to the small Franck-Condon overlap and the weak collective effects. To clarify the influence of the number N of organic molecules on the hybridized frequencies as well as the decay rates, we numerically show the spatial intensity profile of the transmitted field. It is clearly to see that the evolution of the frequency for lower polariton with the number N of molecules obeys the rule given by Eq. (19b) [see green dashed line in Fig. 2(g, h)]. For blue-detuned illumination, the spatial intensity profile of the transmitted field seems more complicated [see Fig. 2(c-h)]. Typically, when the collective coupling strength $g\sqrt{N} > \nu$ for large Franck-Condon overlap (i.e. $\lambda^2 \sim 1$), one more polaritonic peak appears in the cavity transmission profile [see black dotted line Fig. 2(f)]. For the left branch in Fig. 2(h), the relation between the number N of molecules and the central frequency still obeys the rule given in Eq. (19b) [see blue

dashed line in Fig. 2(h)]. This branch corresponds to the upper polaritons. The appearance of the another branch is caused by the perturbation for the excitation state of the vibrational motion, corresponding to the dark polaritonic state [10].

In addition, we would like to point out here the cavity transmitted field can be used to detect the ultra-cold molecules [25]. Considering the presence of rovibrational states, several theoretical studies have modeled one molecule as a several-level system [25, 41]. One can estimate the number of molecules via the frequency separation between upper and lower polaritonic states. In contrast to the previous work [25], the coupling between electronic states and molecular conformation described by HTC model will make the cavity transmitted field become more complicated [see Fig. 2(g-h)]. Particularly for the large Franck-Condon overlap, it will be a challenge task to detect molecules according to the method introduced by Ref. [25] due to the appearance of the peak for dark polaritonic state, and the suppressed intensity for the upper polaritonic state. Notably, a single peak appeared in the spatial intensity profile of the transmitted field when $\Delta_c > 0$, which is associated with the lower polaritons. Considering the relation between the number N of molecules and the central frequency of the lower polaritonic peaks described by Eq. (19b), we can approximately get the number of molecules as $N \approx \omega_-^2/g^2$ [see yellow dotted line in Fig. 2(g, h)].

IV. FLUORESCENCE SPECTRUM

In the previous section, we have analyzed the polaritonic features via the transmission field profile. With the increasing of the number of molecules, qualitatively different phenomena arise while considering the collective behavior for the emitters. On the other hand, the molecules can interact with each

other via the coupling with the quantized cavity field. This will give rise to the modification of the molecular configuration [42], as well as the transition between the electronic ground and excited states. In this section, we will illustrate how the feature is reflected via the fluorescence spectrum.

Before the introduction of fluorescence spectrum, let us first give the definition of the fluctuation operator. Since the expect values for Pauli lowering operator $\langle \sigma_m \rangle_{ss}$ and the cavity field

$\langle a \rangle_{ss}$ have been obtained in steady state given by Eq. (18), one can represent the fluctuation about this steady state by the following operators

$$\begin{aligned}\delta\sigma_m &= \sigma_m - \langle \sigma_m \rangle_{ss}, \\ \delta a &= a - \langle a \rangle_{ss}.\end{aligned}\quad (21)$$

Considering the formal solution for Pauli operator given by Eq. (9), one can easily derive the expression for the autocorrelation function

$$\begin{aligned}\langle \delta\sigma_m^\dagger(t) \delta\sigma_m(t+\tau) \rangle &= -ig \int_t^{t+\tau} dt_1 e^{-(i\Delta+\Gamma_\perp)(t+\tau-t_1)} \langle \delta\sigma_m^\dagger(t) \mathcal{D}_m(t+\tau) \mathcal{D}_m^\dagger(t_1) \rangle_{ss} - \langle \sigma_m \rangle_{ss} \langle \delta\sigma_m^\dagger(t) \rangle \\ &\quad - ig \int_t^{t+\tau} dt_1 e^{-(i\Delta+\Gamma_\perp)(t+\tau-t_1)} \langle \delta\sigma_m^\dagger(t) \mathcal{D}_m(t+\tau) \mathcal{D}_m^\dagger(t_1) \delta a(t_1) \rangle \\ &\quad + e^{-(i\Delta+\Gamma_\perp)\tau} \langle \delta\sigma_m^\dagger(t) \mathcal{D}_m(t+\tau) \mathcal{D}_m^\dagger(t) \sigma_m(t) \rangle.\end{aligned}\quad (22)$$

Under the large vibrational relaxation condition $\gamma \gg \kappa$ and $\gamma \gg \Gamma$, the correlation time for vibrational motion would be much shorter than the timescale of the correlation between cavity field and molecules, as well as the intra-molecule correlations. Therefore, the four-operator correlation functions can be separated as

$$\langle \delta\sigma_m^\dagger(t) \mathcal{D}_m(t+\tau) \mathcal{D}_m^\dagger(t_1) \mathcal{O}(t_1) \rangle \approx \langle \delta\sigma_m^\dagger(t) \mathcal{O}(t_1) \rangle \langle \mathcal{D}_m(t+\tau) \mathcal{D}_m^\dagger(t_1) \rangle \quad (23)$$

with $\mathcal{O}(t)$ in the set $\{a(t), \sigma_m(t), \sigma_n(t)\}$. In the limit of a long time scale, the system would be in the steady state. Then the first line in Eq. (22) can be neglected as the expectation value for fluctuation operator $\langle \delta\sigma_m \rangle_{ss}$ will be zero. The formulation for the desired auto-correlation function is deduced with convolution integral

$$\langle \delta\sigma_m^\dagger(0) \delta\sigma_m(\tau) \rangle_{ss} = -ig \int_0^\infty dt_1 \mathcal{F}_m(\tau - t_1) \langle \delta\sigma_m^\dagger(0) \delta a(t_1) \rangle_{ss} - \langle \delta\sigma_m^\dagger \delta\sigma_m \rangle_{ss} \mathcal{F}_m(\tau), \quad (24)$$

where $\langle \delta\sigma_m^\dagger(0) \delta\mathcal{O}(\tau) \rangle_{ss} \equiv \lim_{t \rightarrow \infty} \langle \delta\sigma_m^\dagger(t) \delta\mathcal{O}(t+\tau) \rangle_{ss}$ and $\langle \delta\sigma_m^\dagger \delta\sigma_m \rangle_{ss} = \langle \sigma_m^\dagger \delta\sigma_m \rangle_{ss} - \langle \delta\sigma_m \rangle_{ss} \langle \sigma_m^\dagger \rangle_{ss}$. Taking the Fourier transformation with the definition $S_{\mathcal{O}}^m(\omega) = \int_{-\infty}^\infty d\tau \langle \delta\sigma_m^\dagger(0) \delta\mathcal{O}(\tau) \rangle_{ss} e^{-i\omega\tau}$, the correlation function given by Eq. (24) can be reformed in the Fourier domain, i.e.,

$$S_{\sigma_m}^m = -\tilde{\mathcal{F}}_m[igS_a^m - \langle \delta\sigma_m^\dagger \delta\sigma_m \rangle_{ss}], \quad (25)$$

where $\tilde{\mathcal{F}}_m(\omega)$ is the Fourier form for the factor $\mathcal{F}_m(t)$.

Taking the similar method, one can respectively get the Fourier forms for the correlation functions $\langle \delta\sigma_m^\dagger(0) \delta\sigma_n(\tau) \rangle_{ss}$ between molecules, and also the correlation function $\langle \delta\sigma_m^\dagger(0) \delta a(\tau) \rangle_{ss}$ between cavity and molecules

$$\begin{aligned}S_{\sigma_n}^m &= -\tilde{\mathcal{F}}_n(igS_a^m - \langle \delta\sigma_m^\dagger \delta\sigma_n \rangle_{ss}), \\ S_a^m &= -ig\tilde{\mathcal{F}}_a\left(\sum_{n \neq m}^N S_{\sigma_n}^m + S_{\sigma_m}^m\right) + \tilde{\mathcal{F}}_a \langle \delta\sigma_m^\dagger \delta a \rangle_{ss},\end{aligned}\quad (26)$$

where $\langle \delta\sigma_m^\dagger \delta\mathcal{O} \rangle_{ss} = \langle \sigma_m^\dagger \mathcal{O} \rangle_{ss} - \langle \mathcal{O} \rangle_{ss} \langle \sigma_m^\dagger \rangle_{ss}$, and $\tilde{\mathcal{F}}_a(\omega) = 1/[i(\Delta_c + \omega) + \kappa]$.

For identical molecules, the functions $S_{\sigma_n}^m$ ($n \neq m$) are same for any molecule pair (m, n) and $S_{\sigma_m}^m$ are interchangeable for any molecule (m). As a result, Eqs. (25-26) can be

simply reformed as

$$\mathcal{M}_s \mathbf{S}_{\text{Vec}} + \mathbf{S}_{\text{in}} = 0, \quad (27)$$

with the coefficient matrix

$$\mathcal{M}_s = \begin{pmatrix} -1 & 0 & -ig\tilde{\mathcal{F}}_m \\ 0 & -1 & -ig\tilde{\mathcal{F}}_n \\ -ig\tilde{\mathcal{F}}_a & -i(N-1)g\tilde{\mathcal{F}}_a & -1 \end{pmatrix},$$

the vector for the Fourier form of correlation functions $\mathbf{S}_{\text{Vec}} = (S_{\sigma_m}^m, S_{\sigma_n}^m, S_a^m)^T$, and the input vector $\mathbf{S}_{\text{in}} = (\tilde{\mathcal{F}}_m \langle \delta\sigma_m^\dagger \delta\sigma_m \rangle_{ss}, \tilde{\mathcal{F}}_n \langle \delta\sigma_m^\dagger \delta\sigma_n \rangle_{ss}, \tilde{\mathcal{F}}_a \langle \delta\sigma_m^\dagger \delta a \rangle_{ss})^T$. To this end, the solution can be obtained via $\mathbf{S}_{\text{Vec}} = -\mathcal{M}_s^{-1} \mathbf{S}_{\text{in}}$. It should be noted that the above equation can also be derived via considering the quantum regression theorem. Different with the traditional methods [43], the convolution integral for $\langle \sigma_m(t) \rangle$ given by Eq. (12) requires us to get the dynamic equation for the correlation function from the perspective of the frequency domain. In addition, to obtain the value of the vector \mathbf{S}_{Vec} , one need to calculate the expectations $\langle \sigma_m^\dagger \mathcal{O} \rangle$ in steady state, which have been discussed in Appendix C.

According to the definition of the collective operator $J_- = \sum_{m=0}^N \sigma_m$, the fluorescence spectrum in steady sit-

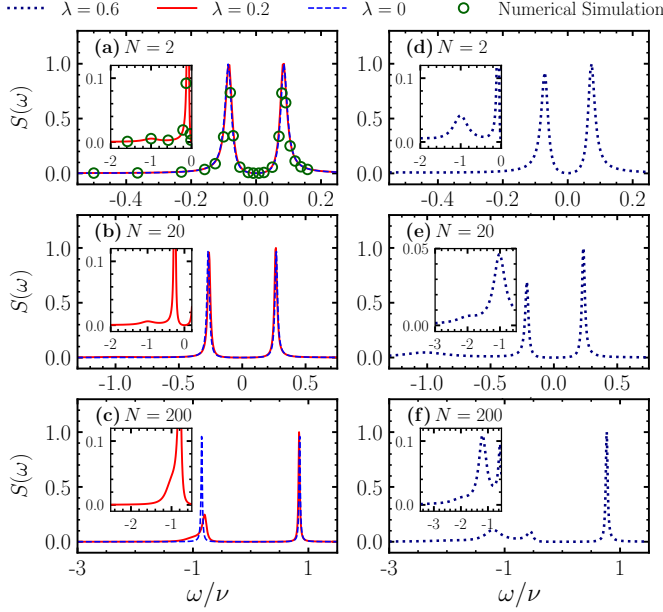


Figure 3. (Colored online) The fluorescence spectrum at resonance $\omega_c = \omega_{00} = \omega_l$ with various number N of organic molecules (increases as 2, 20, and 200). We compare the HTC model for different number N of molecules, against the TC model (blue dashed line) when (a-c) $\lambda = 0.2$ and (d-f) $\lambda = 0.6$. (a) The green circle markers are numerical calculated with the help of QuTiP for the case $\lambda = 0.2$, and $N = 2$. The other parameters are the same with Fig. 2.

uation can be achieved by taking the Fourier transformation $S = \lim_{t \rightarrow \infty} \Re \int_{-\infty}^{\infty} d\tau \langle \delta J_-^\dagger(t) \delta J_-(t+\tau) \rangle e^{-i\omega\tau}$. Since $\langle \delta \sigma_m^\dagger(t) \delta \sigma_m(t+\tau) \rangle$, $\langle \delta \sigma_m^\dagger(t) \delta \sigma_n(t+\tau) \rangle$ ($m \neq n$) are same for all molecules and all molecular pairs respectively, we can further get the relation

$$S = N \Re S_{\sigma_m}^m + N(N-1) \Re S_{\sigma_n}^m. \quad (28)$$

Figure 3 illustrates the fluorescence spectrum at resonance $\omega_c = \omega_{00} = \omega_l$. With the number N of molecules increasing, the spectral weight shows some interesting features. In the limit of $\lambda = 0$, the profile for the fluorescence spectrum will exhibit two symmetric peaks with the central frequencies ω_{\pm} given by Eq. (19b) (see blue dashed line). For finite λ , the coupling between electronic and molecular conformation will bring us more amazing phenomena, e.g. the Stokes scattering, the asymmetric profile for fluorescence spectrum [see red solid line in Fig. 3(a-c) and black dotted line in Fig. 3(d-f)]. When $N = 2$, one more peak at frequency $\omega = -\nu$ appeared compared with TC (i.e. $\lambda = 0$) model [see red solid line in Fig. 3(a) and black dotted line in Fig. 3(d)]. This peak corresponds to the Stokes process $|e\rangle |0\rangle_{\text{vib}} \rightarrow |g\rangle |1\rangle_{\text{vib}}$, with the transition rate characterized by the Franck-Condon factors $_{\text{vib}} \langle 1 | \mathcal{D}(\lambda) | 0 \rangle_{\text{vib}}$ [44]. As the number N of organic molecules increases, the coverage of the Stokes line in the frequency domain will be broadened [see black dotted line in Fig. 3(e, f)]. Especially, at $N = 20$, one can find that another peak appeared at frequency $\omega = -2\nu$, corresponding to the Stoke process $|e\rangle |0\rangle_{\text{vib}} \rightarrow |g\rangle |2\rangle_{\text{vib}}$. The dependence of

the profile for the Stokes line on the number of molecules reflects that the molecular conformation has been modified via the collective behavior. When the collective coupling strength $g\sqrt{N} > \nu$, the contribution of dark polaritonic state should be taken into account [see black dotted line in Fig. 3(f)], which would bring new physics.

V. CONCLUSION

In summary, we have studied the collective behavior for organic molecules based on the HTC model. Via adiabatically eliminating the degree of freedom of the vibrational motion, we have derived a set of linear equations in Laplace (or Fourier) domain, involving the Pauli operators, the correlation between cavity field and molecules, and the correlation between molecules. Based on these equations, we have studied the cavity transmission spectrum for an ensemble of identical organic molecules. Our results reveal that, different with TC model, the coupling between electronic states and molecular conformation will produce additional dephasing as well as the frequency shift for excitons. This will result in some amazing phenomena, e.g. the suppressed upper polaritonic peak, dark polaritonic peak with central frequency slightly changed via increasing the number of molecules. In addition, the cavity transmitted field is suggested to detect the ultra-cold molecules [25]. Considering the relationship between the hybridized frequencies and the number of molecules, one can estimate the number of molecules via the frequency shift for the lower polaritonic state. Moreover, we also study the steady population on the excited state for total molecules and the fluorescence spectrum. With the number of molecules increasing, the coverage of the Stokes line in the frequency domain is broadened. This means that the probabilities for transition from electronic excited state to the vibrational excited states in the electronic ground state increased. In other words, the conformation of molecules will be modified due to the collective effects, providing a potential application in the control of the chemical reactivity [11, 12], energy and charge transport [13, 14], and Förster resonance energy transfer [15–17].

ACKNOWLEDGMENTS

This work was supported by the Natural Science Foundation of China (under Grants No. 12074030 and No. U1930402). Q. Z. acknowledges fruitful discussions with Lei Du, Yong Li and Michael Reitz.

Appendix A: Dynamic of the Vibrational Motion

In the limit of weak probe fields $\eta \ll \kappa$, the Heisenberg-Langevin equation for the vibrational motion is given [17] by

$$\frac{d}{dt} b = -i(\nu - i\gamma)b + \sqrt{2\gamma}b_{\text{in}}, \quad (A1)$$

where b_{in} is the annihilation operator of thermal noise with zero-average value. The non-vanishing correlation functions are

$$\begin{aligned}\langle b_{\text{in}}^\dagger(t)b_{\text{in}}(t_1) \rangle &= \bar{n}_{\text{th}}\delta(t-t_1), \\ \langle b_{\text{in}}(t)b_{\text{in}}^\dagger(t_1) \rangle &= (1+\bar{n}_{\text{th}})\delta(t-t_1),\end{aligned}\quad (\text{A2})$$

where $\bar{n}_{\text{th}} = 1/[\exp(\hbar\nu/k_B T_{\text{vib}})] - 1$ is the average thermal photon numbers at the effective temperature T_{vib} . For brevity, let us assume that the temperature satisfies $k_B T_{\text{vib}}/\hbar\nu \ll 1$. According to the quantum regression theorem [34, 43], the non-zero correlation for the boson operator b at $\tau > 0$ is then obtained

$$\langle b(t)b^\dagger(t+\tau) \rangle = e^{-(i\nu+\gamma)\tau}. \quad (\text{A3})$$

Introducing the momentum operator $p = i(b^\dagger - b)/\sqrt{2}$, one can get its correlation function

$$\langle p(t+\tau)p(t) \rangle = \frac{1}{2}e^{-(i\nu+\gamma)\tau}, \quad (\text{A4})$$

and the variance $\langle p^2 \rangle(t) = 1/2$. Now, we can get the two-time correlation function for displacement operator $\mathcal{D} = \exp[\lambda(b - b^\dagger)] = \exp(i\sqrt{2}\lambda p)$ as

$$\begin{aligned}\langle \mathcal{D}(t+\tau)\mathcal{D}^\dagger(t) \rangle &= \langle e^{i\sqrt{2}\lambda p(t+\tau)}e^{-i\sqrt{2}\lambda p(t)} \rangle, \\ &= \langle e^{i\sqrt{2}\lambda[p(t+\tau)-p(t)]} \rangle e^{\lambda^2[p(t+\tau),p(t)]}, \\ &= \left\langle \sum_k \frac{(i\sqrt{2}\lambda)^k}{k!} [p(t+\tau) - p(t)]^k \right\rangle e^{\lambda^2[p(t+\tau),p(t)]}.\end{aligned}\quad (\text{A5a})$$

Taking use of the Isserlis' theorem [22], one can simplify Eq. (A5a) into

$$\begin{aligned}\langle \mathcal{D}(t+\tau)\mathcal{D}^\dagger(t) \rangle &= e^{-\lambda^2\langle [p(t+\tau)-p(t)]^2 \rangle} e^{\lambda^2[p(t+\tau),p(t)]}, \\ &= e^{-\lambda^2[2\langle p^2 \rangle - 2\langle p(t+\tau)p(t) \rangle]}, \\ &= e^{-\lambda^2} e^{\lambda^2 e^{-(i\nu+\gamma)\tau}}.\end{aligned}\quad (\text{A5b})$$

Similarly, we can also get the four-time correlation function for displacement operator at $t > t_1 > t_2 > t_3$,

$$\begin{aligned}\langle \mathcal{D}(t)\mathcal{D}^\dagger(t_1)\mathcal{D}(t_2)\mathcal{D}^\dagger(t_3) \rangle &= \langle e^{i\sqrt{2}\lambda p(t)}e^{-i\sqrt{2}\lambda p(t_1)}e^{i\sqrt{2}\lambda p(t_2)}e^{-i\sqrt{2}\lambda p(t_3)} \rangle, \\ &= e^{-\lambda^2\langle [p(t)-p(t_1)+p(t_2)-p(t_3)]^2 \rangle} e^{-\lambda^2[p(t)-p(t_1),p(t_2)-p(t_3)]} e^{\lambda^2[p(t),p(t_1)]} e^{\lambda^2[p(t_2),p(t_3)]}, \\ &= e^{-2\lambda^2[2\langle p^2 \rangle - \langle p(t)p(t_1) \rangle + \langle p(t)p(t_2) \rangle - \langle p(t)p(t_3) \rangle - \langle p(t_1)p(t_2) \rangle + \langle p(t_1)p(t_3) \rangle - \langle p(t_2)p(t_3) \rangle]} \\ &= e^{-2\lambda^2} e^{2\lambda^2\langle p(t)p(t_1) \rangle} e^{-2\lambda^2\langle p(t)p(t_2) \rangle} e^{2\lambda^2\langle p(t)p(t_3) \rangle} e^{2\lambda^2\langle p(t_1)p(t_2) \rangle} e^{-2\lambda^2\langle p(t_1)p(t_3) \rangle} e^{2\lambda^2\langle p(t_2)p(t_3) \rangle}.\end{aligned}\quad (\text{A6a})$$

Submitting Eq. (A4) into above equation, and taking the Taylor series expansion, we finally get the expression for the four-time correlation in the sum form

$$\begin{aligned}\langle \mathcal{D}(t)\mathcal{D}^\dagger(t_1)\mathcal{D}(t_2)\mathcal{D}^\dagger(t_3) \rangle &= e^{-2\lambda^2} \sum_{\{k\}} \frac{(-1)^{k_2+k_5} \lambda^{2(k_1+k_2+k_3+k_4+k_5+k_6)}}{\prod_j k_j!} e^{-(k_1+k_2+k_3)(i\nu+\gamma)(t-t_1)} e^{-(k_2+k_3+k_4+k_5)(i\nu+\gamma)(t_1-t_2)} e^{-(k_3+k_5+k_6)(i\nu+\gamma)(t_2-t_3)} \\ &\quad .\end{aligned}\quad (\text{A6b})$$

Appendix B: Dynamic of Electronic States

From the Langevin equation for the cavity field a described by Eq. (8a), we can take the integration with respect of time to get the formal solution

$$a = \int_0^t dt_1 e^{-(i\delta_c+\kappa)(t-t_1)} [-ig \sum_m \sigma_m(t_1) + \eta + (\sqrt{2\kappa_1} + \sqrt{2\kappa_2})a_{\text{in}}(t_1)]. \quad (\text{B1})$$

By plugging Eq. (B1) into the formal solution of the dipole operator $\sigma_m(t)$ described by Eq. (9), and taking the averages, we find

$$\langle \sigma_m \rangle = -ig \int_0^t dt_1 e^{-(i\Delta+\Gamma_\perp)(t-t_1)} \int_0^{t_1} dt_2 e^{-(i\Delta_c+\kappa)(t_1-t_2)} \langle \mathcal{D}_m(t)\mathcal{D}_m^\dagger(t_1) [-ig \sum_{n \neq m}^N \sigma_n(t_2) - ig\sigma_m(t_2) + \eta] \rangle. \quad (\text{B2a})$$

The item $\langle \mathcal{D}_m(t) \mathcal{D}_m^\dagger(t_1) \sigma_n(t) \rangle$ reflects the induced interaction between m -th and n -th molecule via the quantized cavity field. The item $\langle \mathcal{D}_m(t) \mathcal{D}_m^\dagger(t_1) \sigma_m(t_1) \rangle$ relates to the modification of the frequency and decay rate. When we considering the evolution for the Pauli operators, and submitting Eq. (9) into Eq. (B2a), the average value for Pauli operator is given by

$$\begin{aligned} \langle \sigma_m \rangle = & ig^3 \sum_{n \neq m}^N \int_0^t dt_1 e^{-(i\Delta + \Gamma_\perp)(t-t_1)} \int_0^{t_1} dt_2 e^{-(i\Delta_c + \kappa)(t_1-t_2)} \int_0^{t_2} dt_3 e^{-(i\Delta + \Gamma_\perp)(t_2-t_3)} \langle \mathcal{D}_m(t) \mathcal{D}_m^\dagger(t_1) \mathcal{D}_n(t_2) \mathcal{D}_n^\dagger(t_3) a(t_3) \rangle \\ & + ig^3 \int_0^t dt_1 e^{-(i\Delta + \Gamma_\perp)(t-t_1)} \int_0^{t_1} dt_2 e^{-(i\Delta_c + \kappa)(t_1-t_2)} \int_0^{t_2} dt_3 e^{-(i\Delta + \Gamma_\perp)(t_2-t_3)} \langle \mathcal{D}_m(t) \mathcal{D}_m^\dagger(t_1) \mathcal{D}_m(t_2) \mathcal{D}_m^\dagger(t_3) a(t_3) \rangle \\ & - \eta g \int_0^t dt_1 e^{-(i\Delta + \Gamma_\perp)(t-t_1)} \mathcal{D}_m(t) \mathcal{D}_m^\dagger(t_1) \int_0^{t_1} dt_2 e^{-(i\Delta_c + \kappa)(t_1-t_2)}. \end{aligned} \quad (\text{B2b})$$

In the main text, we have roughly take the Markov approximation (under the large vibrational relaxation condition $\gamma \gg \kappa, \gamma$) to separate the degrees of freedom for cavity field and vibrational motion as

$$\langle \mathcal{D}_m(t) \mathcal{D}_m^\dagger(t_1) a(t_1) \rangle \approx \langle \mathcal{D}_m(t) \mathcal{D}_m^\dagger(t_1) \rangle \langle a(t_1) \rangle, \quad (\text{B3a})$$

and also the degrees of freedom for Pauli operator and vibrational motion as

$$\langle \mathcal{D}_m(t) \mathcal{D}_m^\dagger(t_1) \sigma_n(t_1) \rangle \approx \langle \mathcal{D}_m(t) \mathcal{D}_m^\dagger(t_1) \rangle \langle \sigma_n(t_1) \rangle. \quad (\text{B3b})$$

This approach implies that we have roughly take the following approximation

$$\langle \mathcal{D}_m(t) \mathcal{D}_m^\dagger(t_1) \mathcal{D}_m(t_2) \mathcal{D}_m^\dagger(t_3) \rangle \approx \langle \mathcal{D}_m(t) \mathcal{D}_m^\dagger(t_1) \rangle \langle \mathcal{D}_m(t_2) \mathcal{D}_m^\dagger(t_3) \rangle. \quad (\text{B4})$$

In this case, all the displacement operators refer to the same vibrational mode. To test the feasibility of this approximation, we make a further study. According to the expression for the four-time correlation of the displacement operator in Eq. (A6a), we can take the Laplace transformation for Eq. (B2b) to obtain

$$\langle \bar{\sigma}_m \rangle = ig^3 \sum_{n \neq m} \frac{\bar{\mathcal{F}}_m \bar{\mathcal{F}}_n}{i\Delta_c + \kappa} \langle \bar{a} \rangle + ig^3 \bar{\mathcal{F}}_{2,m} \langle \bar{a} \rangle - i\eta g \frac{\bar{\mathcal{F}}_m}{s[i\Delta_c + \kappa]}, \quad (\text{B5})$$

where $\bar{\mathcal{F}}_n = \bar{\mathcal{F}}_n$ for identical molecules, and

$$\begin{aligned} \bar{\mathcal{F}}_{2,m} = & \sum_{\{k\}} \frac{1}{\prod_j k_j!} e^{-2\lambda^2} (-1)^{k_2+k_5} \lambda^{2(k_1+k_2+k_3+k_4+k_5+k_6)} \\ & \times \frac{1}{[s + i\Delta + i(k_1 + k_2 + k_3)\nu + (k_1 + k_2 + k_3)\gamma + \Gamma_\perp][\cdots(1)\cdots][s + i\Delta + i(k_1 + k_2 + k_3)\nu + (k_1 + k_2 + k_3)\gamma + \Gamma_\perp]} \end{aligned} \quad (\text{B6})$$

with $[\cdots(1)\cdots] = [s + i\Delta_c + i(k_2 + k_3 + k_4 + k_5)\nu + (k_2 + k_3 + k_4 + k_5)\gamma + \kappa]$.

Considering the Laplace form of the cavity field described by Eq. (16), and using the final value theorem, we finally get

$$\begin{aligned} \langle a \rangle'_{ss} = & \frac{\eta \mathcal{F}_c^0 (-1 + Ng^2 \mathcal{F}_c^0 \mathcal{F}_m^0)}{-1 + Ng^4 \mathcal{F}_c^0 [\mathcal{F}_{2,m}^0 + (N-1) \mathcal{F}_c^0 (\mathcal{F}_m^0)^2]}, \\ \langle \sigma_m \rangle'_{ss} = & -i\eta g \frac{g^2 \mathcal{F}_c^0 [\mathcal{F}_{2,m}^0 + (N-1) \mathcal{F}_c^0 (\mathcal{F}_m^0)^2] - \mathcal{F}_c^0 \mathcal{F}_m^0}{-1 + Ng^4 \mathcal{F}_c^0 [\mathcal{F}_{2,m}^0 + (N-1) \mathcal{F}_c^0 (\mathcal{F}_m^0)^2]}. \end{aligned} \quad (\text{B7})$$

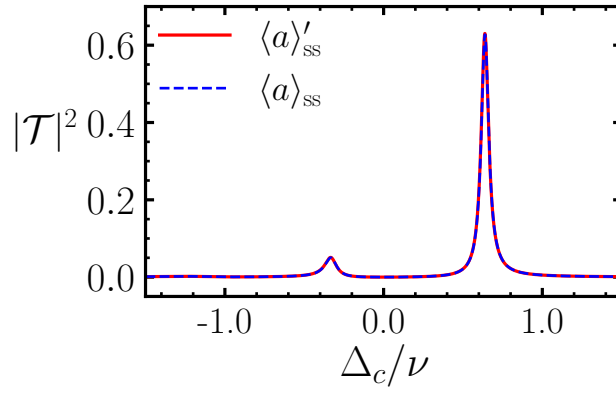


Figure 4. (Colored online) Cavity transmission at resonance $\omega_c = \omega_{00}$ as a function of the detuning Δ_c/ν with the number $N = 200$ of organic molecules at $\lambda = 1$. The data is calculated according to Eq. (B7) (see red solid line) and Eq. (18b) (see blue dashed line), respectively. The other parameters are the same with Fig. (2).

To verify the validity of the Markov approximation to adiabatically eliminate the degree of freedom of vibrational motion, we plot the cavity transmission spectrum at resonance $\omega_c = \omega_{00}$ with the number $N = 200$ of organic molecules at $\lambda = 1$. As illustrated by Fig. 4, we can observe that same behaviors performed when we consider the four-time correlation (see red solid line) or just the two-time correlation (see blue dashed line).

Appendix C: Steady Population

1. Dynamics

From the Heisenberg-Langevin equation in Eq. (7) (or the master equation in Eq. (6), we can derive the dynamical equations for average number of photons in cavity $\langle n_c \rangle = \langle a^\dagger a \rangle$, and the excited state population for m -th dye molecule $\langle P_m \rangle = \langle \sigma_m^\dagger \sigma_m \rangle$

$$\frac{d}{dt} \langle P_m \rangle = -\Gamma_{\parallel} \langle P_m \rangle - ig(\langle a \sigma_m^\dagger \rangle - \langle a^\dagger \sigma_m \rangle), \quad (\text{C1a})$$

$$\frac{d}{dt} \langle n_c \rangle = -2\kappa \langle n_c \rangle - ig \sum_m^N (\langle a^\dagger \sigma_m \rangle - \langle a \sigma_m^\dagger \rangle) + \eta(\langle a \rangle + \langle a^\dagger \rangle), \quad (\text{C1b})$$

where $\Gamma_{\parallel} = 2\Gamma$ is the longitudinal relaxation rate. By taking Laplace transformations for Eq. (C1), we will have the results

$$s \langle \bar{P}_m \rangle = -\Gamma_{\parallel} \langle \bar{P}_m \rangle - ig(\langle \bar{a} \sigma_m^\dagger \rangle - \langle \bar{a}^\dagger \sigma_m \rangle), \quad (\text{C2a})$$

$$s \langle \bar{n}_c \rangle = -2\kappa \langle \bar{n}_c \rangle - ig \sum_m^N (\langle \bar{a}^\dagger \sigma_m \rangle - \langle \bar{a} \sigma_m^\dagger \rangle) + \eta(\langle \bar{a} \rangle + \langle \bar{a}^\dagger \rangle). \quad (\text{C2b})$$

The presence of the operator $a^\dagger \sigma_m$ in Eq. (C2), relates to the nonlinear behavior of the HTC model. In the limit of weak driving $\eta \ll \kappa$, the cavity field in steady situation is approximately in vacuum. Under this situation, the noise correlation between cavity field and the molecules as well as the noise correlation between molecules will play important roles. Therefore, we have to give the dynamics equations for the operator $a^\dagger \sigma_m$. While considering the coupling between the electronic states and molecular conformation, we start from the Langevin equation for the cavity field operator a and the polarized operator $\tilde{\sigma}_m$ as given in Eq. (8), to derive the dynamic equation for $a^\dagger \tilde{\sigma}_m$

$$\begin{aligned} \frac{d}{dt} a^\dagger \tilde{\sigma}_m &= \left(\frac{d}{dt} a^\dagger \right) \tilde{\sigma}_m + a^\dagger \frac{d}{dt} \tilde{\sigma}_m \\ &= [i(\Delta_c - \Delta) - (\kappa + \Gamma_{\perp})] a^\dagger \tilde{\sigma}_m + ig \mathcal{D}_m^\dagger (\sigma_m^\dagger \sigma_m - a^\dagger a) + ig \mathcal{D}_m^\dagger \sum_{n \neq m}^N \sigma_n^\dagger \sigma_m + \sqrt{2\kappa} A_{in}^\dagger \tilde{\sigma}_m + \sqrt{2\Gamma_{\perp}} \mathcal{D}_m^\dagger a^\dagger \sigma_m^{\text{in}}. \end{aligned} \quad (\text{C3a})$$

Integrating with respect to the time t on both sides of Eq. (C3a), then the formal solution for the operator $a^\dagger \sigma_m$ will be obtained

$$a^\dagger \sigma_m = \int_0^t dt_1 e^{[i(\Delta_c - \Delta) - (\kappa + \Gamma_\perp)](t-t_1)} \mathcal{D}_m(t) \mathcal{D}_m^\dagger(t_1) \{ig[P_m(t_1) - n_c(t_1)] + \eta \sigma_m(t_1)\} + \mathcal{X}_{m,\text{ind}}^t + \mathcal{X}_{m,\text{in}}^t, \quad (\text{C3b})$$

with the dipole-dipole term

$$\mathcal{X}_{m,\text{d-d}}^t = ig \int_0^t dt_1 e^{[i(\Delta_c - \Delta) - (\kappa + \Gamma_\perp)](t-t_1)} \mathcal{D}_m(t) \mathcal{D}_m^\dagger(t_1) \sum_{n \neq m}^N \sigma_n^\dagger \sigma_m(t_1), \quad (\text{C3c})$$

and the noise term

$$\mathcal{X}_{\text{in}}^t = \int_0^t dt_1 e^{[i(\Delta_c - \Delta) - (\kappa + \Gamma_\perp)](t-t_1)} \mathcal{D}_m(t) \mathcal{D}_m^\dagger(t_1) [\sqrt{2\kappa} a_{\text{in}}^\dagger \sigma_m(t_1) + \sqrt{2\Gamma_\perp} \mathcal{D}_m^\dagger a^\dagger \sigma_m^{\text{in}}(t_1)]. \quad (\text{C3d})$$

Since these individuals molecules are introduced to couple a quantized cavity field, an efficient interaction between molecules will be induced as described by Eq. (C3c). To find the expression of the dipole-dipole term $\mathcal{X}_{m,\text{d-d}}^t$, one need to consider the expression of $\sigma_n^\dagger \sigma_m$, which can be derived through the following Langevin equation

$$\frac{d}{dt} \tilde{\sigma}_n^\dagger \tilde{\sigma}_m = -2\Gamma_\perp \tilde{\sigma}_n^\dagger \tilde{\sigma}_m + ig \mathcal{D}_m^\dagger \mathcal{D}_n (a^\dagger \sigma_m - a \sigma_n^\dagger) + \sqrt{2\Gamma_\perp} \mathcal{D}_m^\dagger \mathcal{D}_n (\sigma_n^\dagger \sigma_m^{\text{in}} + \sigma_n^{\text{in}\dagger} \sigma_m). \quad (\text{C4a})$$

The evolution of $\sigma_n^\dagger \sigma_m(t)$ is then similarly obtained as

$$\sigma_n^\dagger \sigma_m = ig \int_0^t dt_1 e^{-2\Gamma_\perp(t-t_1)} \mathcal{D}_m(t) \mathcal{D}_m^\dagger(t_1) [a^\dagger \sigma_m(t_1) - a \sigma_n^\dagger(t_1)] \mathcal{D}_n(t_1) \mathcal{D}_n^\dagger(t) + \mathcal{Y}_{\text{in}}^t, \quad (\text{C4b})$$

with the noise term

$$\mathcal{Y}_{\text{in}}^t = \sqrt{2\Gamma_\perp} \int_0^t dt_1 e^{-2\Gamma_\perp(t-t_1)} \mathcal{D}_m(t) \mathcal{D}_m^\dagger(t_1) [\sigma_n^\dagger \sigma_m^{\text{in}}(t_1) + \sigma_n^{\text{in}\dagger} \sigma_m(t_1)] \mathcal{D}_n(t_1) \mathcal{D}_n^\dagger(t). \quad (\text{C4c})$$

From now on, the formal solution for the interactions between cavity and molecules characterized by Eq. (C3b) as well as the interactions between molecules depicted by Eq. (C4b) have been obtained. To get the excited state population for total molecules, one can take the Markov approximation to adiabatically eliminate the vibrational motion without (or with) submitting Eq. (C4b) into Eq. (C3b), which relates to the perturbative treatment in the first (or second) order.

2. Perturbative Treatment in the 1st Order

In this subsection, let us take the perturbative treatment in the first order. Under the Markov approximation with the large vibrational relaxation, we can adiabatically eliminate the vibrational motion as introduced in Sec. II to get the dynamic equations for the item $\langle a^\dagger \sigma_m \rangle$ and $\langle \sigma_n^\dagger \sigma_m \rangle$ in Laplace space

$$\langle \overline{a^\dagger \sigma_m} \rangle = ig \bar{\mathcal{F}}'_m (\langle \bar{P}_m \rangle - \langle \bar{n}_c \rangle) + \sum_{n \neq m}^N \langle \overline{\sigma_n^\dagger \sigma_m} \rangle + \eta \bar{\mathcal{F}}'_m \langle \bar{\sigma}_m \rangle \quad (\text{C5a})$$

$$\langle \overline{\sigma_n^\dagger \sigma_m} \rangle = ig \bar{\mathcal{F}}_{mn} (\langle \overline{a^\dagger \sigma_m} \rangle - \langle \overline{a \sigma_n^\dagger} \rangle), \quad (\text{C5b})$$

where $\bar{\mathcal{F}}'_m$ is the Laplace form for $\mathcal{F}'_m(t) = \exp[i(\Delta_c - i\Delta - \kappa - \Gamma_\perp)t] \langle \mathcal{D}_m(t) \mathcal{D}_m^\dagger(0) \rangle$ with the expression

$$\bar{\mathcal{F}}'_m = \sum_k \frac{\lambda^{2k}}{k!} \frac{e^{-\lambda^2}}{s + i(\Delta - \Delta_c + k\nu) + (\kappa + \Gamma_\perp + k\gamma)}, \quad (\text{C6})$$

and $\bar{\mathcal{F}}_{mn}$ is the Laplace form for $\mathcal{F}_{mn}(t) = \exp(-2\Gamma_\perp t) \langle \mathcal{D}_m(t) \mathcal{D}_m^\dagger(0) \rangle \langle \mathcal{D}_n(0) \mathcal{D}_n^\dagger(t) \rangle$ with the expression

$$\bar{\mathcal{F}}_{mn} = \sum_{k_m, k_n} \frac{\lambda^{2(k_m + k_n)}}{k_m! k_n!} \frac{e^{-2\lambda^2}}{s + i(k_m - k_n)\nu + [2\Gamma_\perp + (k_m + k_n)\gamma]}. \quad (\text{C7})$$

For identical molecules, the Laplace forms for the population of the excited electric state $\overline{\langle \sigma_m^\dagger \sigma_m \rangle}$, the expect value for the interaction between cavity and molecule $\overline{\langle a^\dagger \sigma_m \rangle}$ as well as the function $\bar{\mathcal{F}}'_m$ are the same with that for any molecule (m), and the expect value for the intra-molecule interaction $\overline{\langle \sigma_n^\dagger \sigma_m \rangle}$, as well as the function $\bar{\mathcal{F}}_{mn}$ are the same for any molecule pair (m, n). As a result, we can simplify Eqs. (C2), and (C5), and transform them into matrix form

$$\mathcal{M}_1 \mathbf{V}_1 + \eta \mathbf{V}_{1,\text{in}} = 0, \quad (\text{C8})$$

with the drift matrix

$$\mathcal{M}_1 = \begin{pmatrix} -2\kappa - s & iNg & -iNg & 0 & 0 \\ ig\bar{\mathcal{F}}_m'^* & -1 & 0 & -ig\bar{\mathcal{F}}_m'^* & -i(N-1)g\bar{\mathcal{F}}_m'^* \\ -ig\bar{\mathcal{F}}_m' & 0 & -1 & ig\bar{\mathcal{F}}_m' & i(N-1)g\bar{\mathcal{F}}_m' \\ 0 & -ig & ig & -\Gamma_{\parallel} - s & 0 \\ 0 & -ig\bar{\mathcal{F}}_{mn} & ig\bar{\mathcal{F}}_{mn} & 0 & -1 \end{pmatrix}, \quad (\text{C9})$$

the vector $\mathbf{V}_1 = (\langle \bar{n}_c \rangle, \overline{\langle a\sigma_m^\dagger \rangle}, \overline{\langle a^\dagger \sigma_m \rangle}, \langle \bar{P}_m \rangle, \overline{\langle \sigma_m^\dagger \sigma_n \rangle})^T$ and the input vector $\mathbf{V}_{1,\text{in}} = (\langle \bar{a} \rangle + \langle \bar{a}^\dagger \rangle, \bar{\mathcal{F}}_m'^* \langle \bar{\sigma}_m^\dagger \rangle, \bar{\mathcal{F}}_m' \langle \bar{\sigma}_m \rangle, 0, 0)^T$.

We then obtain the solutions $\mathbf{V}_1 = -\eta \mathcal{M}_1^{-1} \mathbf{V}_{1,\text{in}}$ by direct matrix inversion. According to the final value theorem, the excited state population for all molecules is finally given by

$$\mathcal{P}_N = \sum_{n=1}^N \langle P_m \rangle. \quad (\text{C10})$$

If we set $N = 1$, there will be only one molecule couples to the cavity and the inter-molecule interaction induced by cavity [depicted by Eq. (C3c)] can be neglected. In such situation, the expect value for excited state population in steady state will be simplified as

$$\mathcal{P}_1 = \frac{\eta g^2 \Re \langle a \rangle_{\text{ss}} \Re \mathcal{F}_m'^0 - \eta g \kappa \Im \{ \mathcal{F}_m'^0 \langle \sigma_m \rangle_{\text{ss}} \}}{\Gamma \kappa + g^2 (\Gamma + \kappa) \Re \mathcal{F}_m'^0}, \quad (\text{C11})$$

where $\mathcal{F}_m'^0 = \lim_{s \rightarrow 0} \bar{\mathcal{F}}_m'$.

Figure 5 illustrates the excited state population for all molecules at resonance $\omega_c = \omega_{00}$ with and without the incoherent coupling between molecules. We compare the HTC model (red solid line) for varying number of molecule N , against the TC model (blue dashed line) in the limit $\alpha = 0$ (a-d) and $\alpha = 1$ (e-h). For finite λ , the transfer rate of population from upper polaritonic states to lower polaritonic states and dark polaritonic states increased with the number of organic molecules increasing. Consequently the population for upper polaritonic states will be reduced, and the population for dark polaritonic states is going to be increased. In addition, the transfer rate for the anti-Stokes process $|g\rangle |0\rangle_{\text{vib}} \rightarrow |e\rangle |1\rangle_{\text{vib}}$ is enhanced with the increasing of the number N of organic molecules. This reflects that the molecular conformation has been modified via the collective behavior.

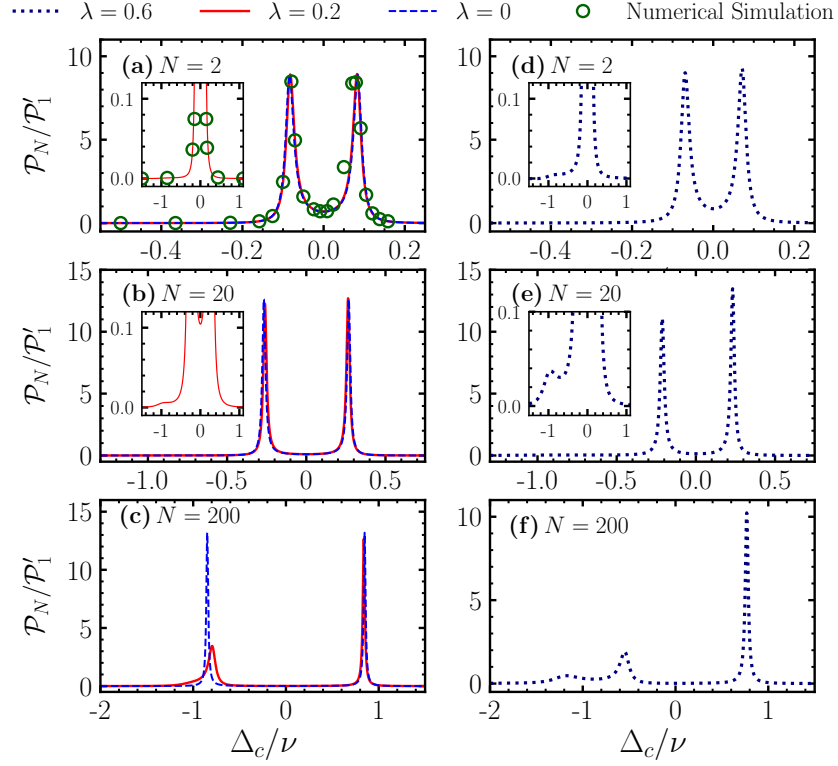


Figure 5. (Colored online) Steady population. The excited state population for all molecules at $\omega_c = \omega_{00}$ in steady state as a function of the detuning Δ_c/ν with different number N (increases as 2, 20 and 200) of organic molecules at $\lambda = 0.6$ (red solid line) and $\lambda = 0$ (blue dashed line) when (a-c) $\alpha = 0$ and (d-f) $\alpha = 1$. (a, d) The black dotted line shows the numerical simulation results for the case $\lambda = 0.6$, $N = 2$ with the help of QuTiP. P'_1 is the unit value given by Eq. (C11) at $\Delta = 0$, $\lambda = 0$. The other parameters are the same with Fig. 2.

3. Perturbative Treatment in the 2nd Order

To test the reasonableness of the approximation as previously mentioned, we will take perturbative treatment in higher order. Substituting Eq. (C4b) into Eq. (C3c), and taking the averages, we find

$$\begin{aligned} \langle \mathcal{X}_{m,d-d}^t \rangle &\approx -g^2 \sum_{n \neq m}^N \int_0^t dt_1 e^{[i(\Delta_c - \Delta) - (\kappa + \Gamma_\perp)](t-t_1)} \int_0^{t_1} dt_2 e^{-2\Gamma_\perp(t_1-t_2)} \langle \mathcal{D}_m(t) \mathcal{D}_m^\dagger(t_2) \rangle \langle \mathcal{D}_n(t_2) \mathcal{D}_n^\dagger(t_1) \rangle \\ &\quad \times [\langle a^\dagger \sigma_m \rangle(t_2) - \langle a \sigma_n^\dagger \rangle(t_2)], \end{aligned} \quad (C12)$$

Here we have adiabatically eliminated the vibrational motion under the large vibrational relaxation condition (i.e. $\gamma \gg \kappa$ and $\gamma \gg \Gamma$). Noticing that the correlation function $\langle \mathcal{D}_m(t) \mathcal{D}_m^\dagger(t_2) \rangle$ (and $\langle \mathcal{D}_m(t) \mathcal{D}_m^\dagger(t_1) \rangle$) depends on the time difference $t - t_2$ (and $t - t_1$) as described in Eq. (13), we can reform Eq. (C12) as

$$\begin{aligned} \langle \mathcal{X}_{m,ind}^t \rangle &= -g^2 e^{-\lambda^2} \sum_{n \neq m}^N \int_0^t dt_1 e^{[i(\Delta_c - \Delta) - (\kappa + \Gamma_\perp)](t-t_1)} \int_0^{t_1} dt_2 e^{-2\Gamma_\perp(t_1-t_2)} e^{\lambda^2 e^{-(\gamma+i\nu)(t-t_2)}} \langle \mathcal{D}_n(t_2) \mathcal{D}_n^\dagger(t_1) \rangle \\ &\quad \times [\langle a^\dagger \sigma_m \rangle(t_2) - \langle a \sigma_n^\dagger \rangle(t_2)]. \\ &= -g^2 \sum_{n \neq m}^N \sum_k \int_0^\infty dt_1 \int_0^\infty dt_2 \mathcal{F}_m^{(k)}(t-t_1) \mathcal{F}_{mn}^{(k)}(t_1-t_2) [\langle a^\dagger \sigma_m \rangle(t_2) - \langle a \sigma_n^\dagger \rangle(t_2)], \end{aligned} \quad (C13)$$

where $\tilde{\Delta}_k = \Delta_c - \Delta + k\nu$, $\tilde{\Gamma}_{1,k} = \kappa + \Gamma_\perp + k\gamma$, $\tilde{\Gamma}_{2,k} = 2\Gamma_\perp + k\gamma$, $\mathcal{F}_m^{(k)}(t) = \Theta(t) \lambda^{2k} \exp(-\lambda^2) \exp[(i\tilde{\Delta}_k - \tilde{\Gamma}_{1,k})t]/k!$, and $\mathcal{F}_{mn}^{(k)}(t_1-t_2) = \Theta(t_1-t_2) \exp[-(ik\nu + \tilde{\Gamma}_{2,k})(t_1-t_2)] \langle \mathcal{D}_n(t_2) \mathcal{D}_n^\dagger(t_1) \rangle$. Since Eq. (C13) represents a convolution, one can

take use the Laplace transformation to rewritten Eq. (C12) into the Laplace space:

$$\langle \bar{\mathcal{X}}_{m,\text{ind}}^t \rangle = -g^2 \sum_{n \neq m}^N \bar{\mathcal{F}}_{mn} [\langle \bar{a}^\dagger \sigma_m \rangle - \langle \bar{a} \sigma_n^\dagger \rangle], \quad (\text{C14})$$

where

$$\begin{aligned} \bar{\mathcal{F}}_{mn} &= \sum_k \bar{\mathcal{F}}_m^{(k)} \bar{\mathcal{F}}_{mn}^{(k)}, \\ &= \sum_{k_m, k_n} \frac{\lambda^{2(k_m + k_n)}}{k_m! k_n!} \frac{e^{-2\lambda^2}}{[s + i(\Delta - \Delta_c + k_m \nu) + (\kappa + \Gamma_\perp + k_m \gamma)][s + i(k_m - k_n) \nu + 2\Gamma_\perp + (k_m + k_n) \gamma]}. \end{aligned} \quad (\text{C15})$$

Via substituting Eq. (9) into Eq. (C3b), and adiabatically eliminating the degree of freedom of vibrational motion, we similarly obtain the evolution of $\langle \bar{a}^\dagger \sigma_m \rangle$ in Laplace space

$$\langle \bar{a}^\dagger \sigma_m \rangle = ig[\bar{\mathcal{F}}'_m(\langle \bar{P}_m \rangle - \langle \bar{n}_c \rangle) - \eta \bar{\mathcal{F}}'_{cm} \langle \bar{a} \rangle] - g^2 \sum_{n \neq m}^N \bar{\mathcal{F}}_{mn} [\langle \bar{a}^\dagger \sigma_m \rangle - \langle \bar{a} \sigma_n^\dagger \rangle], \quad (\text{C16})$$

where $\bar{\mathcal{F}}'_m$ is the Laplace form for $\mathcal{F}'_m(t) = \exp[(i\Delta_c - i\Delta - \kappa - \Gamma_\perp)t] \langle \mathcal{D}_m(t) \mathcal{D}_m^\dagger(0) \rangle$ with the expression

$$\bar{\mathcal{F}}'_m = \sum_k \frac{\lambda^{2k}}{k!} \frac{e^{-\lambda^2}}{s + i(\Delta - \Delta_c + k\nu) + (\kappa + \Gamma_\perp + k\gamma)}, \quad (\text{C17})$$

and

$$\bar{\mathcal{F}}'_{cm} = \sum_k \frac{\lambda^{2k}}{k!} \frac{e^{-\lambda^2}}{[s + i(\Delta - \Delta_c + k\nu) + (\kappa + \Gamma_\perp + k\gamma)][s + i(\Delta + k\nu) + (\Gamma_\perp + k\gamma)]}. \quad (\text{C18})$$

For identical molecules, the Laplace forms for the population of the excited electric state $\langle \bar{\sigma}_m^\dagger \sigma_m \rangle$, the expect value for the interaction between cavity and molecule $\langle \bar{a}^\dagger \sigma_m \rangle$ as well as the function $\bar{\mathcal{F}}'_m$ are the same with that for any molecule (m), and the expect value for the intra-molecule interaction $\langle \bar{\sigma}_n^\dagger \sigma_m \rangle$, as well as the function $\bar{\mathcal{F}}_{mn}$ are the same for any molecule pair (m, n). As a result, we can simplify Eqs. (C2), and (C16) into matrix form

$$\mathcal{M}_2 \mathbf{V}_2 + \eta \mathbf{V}_{2,\text{in}} = 0, \quad (\text{C19})$$

with the drift matrix

$$\mathcal{M}_2 = \begin{pmatrix} -2\kappa - s & -iNg & iNg & 0 \\ -ig\bar{\mathcal{F}}'_m & -(N-1)g^2\bar{\mathcal{F}}_{mn} - 1 & (N-1)g^2\bar{\mathcal{F}}_{mn} & ig\bar{\mathcal{F}}'_m \\ ig\bar{\mathcal{F}}'^*_m & (N-1)g^2\bar{\mathcal{F}}'^*_{mn} & -(N-1)g^2\bar{\mathcal{F}}'^*_{mn} - 1 & -ig\bar{\mathcal{F}}'^*_m \\ 0 & ig & -ig & -\Gamma_\parallel - s \end{pmatrix}, \quad (\text{C20})$$

the vector $\mathbf{V}_2 = (\langle \bar{n}_c \rangle, \langle \bar{a}^\dagger \sigma_m \rangle, \langle \bar{a} \sigma_m^\dagger \rangle, \langle \bar{P}_m \rangle)^T$ and the input vector $\mathbf{V}_{2,\text{in}} = (\langle \bar{a} \rangle + \langle \bar{a}^\dagger \rangle, -ig\bar{\mathcal{F}}'_{cm} \langle \bar{a} \rangle, ig\bar{\mathcal{F}}'^*_{cm} \langle \bar{a}^\dagger \rangle, 0)^T$. We then obtain the solutions $\mathbf{V}_2 = -\eta \mathcal{M}_2^{-1} \mathbf{V}_{2,\text{in}}$ by direct matrix inversion. Finally, the excited state population for total molecules is given

$$\mathcal{P}''_N = \sum_{n=1}^N \langle P_m \rangle. \quad (\text{C21})$$

If we set $N = 1$, the expect value for excited state population in steady state will be simplified as

$$\mathcal{P}''_1 = \eta g^2 \frac{\Re \langle a \rangle_{ss} \Re \mathcal{F}_m'^0 + \kappa \Re \{ \mathcal{F}_{cm}'^0 \langle a \rangle_{ss} \}}{\Gamma \kappa + g^2 (\Gamma + \kappa) \Re \mathcal{F}_m'^0}, \quad (\text{C22})$$

where $\mathcal{F}_m'^0 = \lim_{s \rightarrow 0} \bar{\mathcal{F}}'_m$, and $\mathcal{F}_{cm}'^0 = \lim_{s \rightarrow 0} \bar{\mathcal{F}}'_{cm}$.

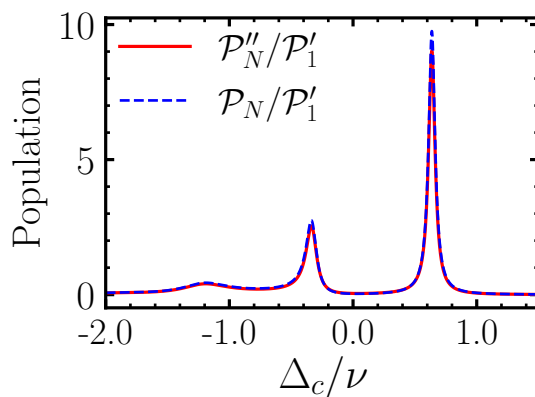


Figure 6. (Colored online) Steady population. The excited state population for total molecules at $\omega_c = \omega_{00}$ in steady state as a function of the detuning Δ_c/ν with the number $N = 200$ of organic molecules at $\lambda = 1$. We compare the perturbative method in 1st order (blue dashed line) against the 2nd order (red solid line). P'_1 is the unit value given by Eq. (C11) at $\Delta = 0$, $\lambda = 0$. The other parameters are the same with Fig. 2.

To test the reasonableness of the Markov approximation to adiabatically eliminate the degree of freedom for the vibrational motion, we plot the excited steady population for total molecules various the detuning Δ_c/ν at $\omega_c = \omega_{00}$ with the number $N = 200$ of organic molecules at $\lambda = 1$. We can observe that similar behaviors performed when we take the perturbative method in second order (see red solid line) and first order (see blue dashed line).

-
- [1] M. Klessinger and J. Michl, *Excited States and Photo-Chemistry of Organic Molecules*, (Wiley, 1995).
 - [2] R. F. Aroca, *Phys. Chem. Chem. Phys.* **15**, 5355 (2013).
 - [3] B. Doppagne, M. C. Chong, E. Lorchat, S. Berciaud, M. Romeo, H. Bulou, A. Boeglin, F. Scheurer, and G. Schull, *Phys. Rev. Lett.* **118**, 127401 (2017).
 - [4] G. Wrigge, I. Gerhardt, J. Hwang, G. Zumofen, and V. Sandoghdar, *Nat. Phys.* **4**, 60 (2008).
 - [5] S. Kühn, U. Håkanson, L. Rogobete, and V. Sandoghdar, *Phys. Rev. Lett.* **97**, 017402 (2006).
 - [6] D. G. Lidzey, D. D. C. Bradley, M. S. Skolnick, T. Virgili, S. Walker, and D. M. Whittaker, *Nature* **395**, 53 (1998).
 - [7] R. Holmes and S. Forrest, *Org. Electron.* **8**, 77 (2007).
 - [8] J. R. Tischler, M. S. Bradley, V. Bulović, J. H. Song, and A. Nurmikko, *Phys. Rev. Lett.* **95**, 036401 (2005).
 - [9] S. Kéna-Cohen, M. Davanço, and S. R. Forrest, *Phys. Rev. Lett.* **101**, 116401 (2008).
 - [10] F. Herrera and J. Owrutsky, *J. Chem. Phys.* **152**, 100902 (2020).
 - [11] F. Herrera and F. C. Spano, *Phys. Rev. Lett.* **116**, 238301 (2016).
 - [12] M. Du, R. F. Ribeiro, and J. Yuen-Zhou, *Chem* **5**, 1167 (2019).
 - [13] J. Schachenmayer, C. Genes, E. Tignone, and G. Pupillo, *Phys. Rev. Lett.* **114**, 196403 (2015).
 - [14] D. Hagenmüller, J. Schachenmayer, S. Schütz, C. Genes, and G. Pupillo, *Phys. Rev. Lett.* **119**, 223601 (2017).
 - [15] X. Zhong, T. Chervy, S. Wang, J. George, A. Thomas, J. A. Hutchison, E. Devaux, C. Genet, and T. W. Ebbesen, *Angew. Chem. Int. Edit.* **55**, 6202 (2016).
 - [16] M. Reitz, F. Mineo, and C. Genes, *Scientific Reports* **8**, 9050 (2018).
 - [17] M. Reitz, C. Sommer, and C. Genes, *Phys. Rev. Lett.* **122**, 203602 (2019).
 - [18] M. A. Zeb, P. G. Kirton, and J. Keeling, *ACS Photonics* **5**, 249 (2018).
 - [19] J. Klaers, J. Schmitt, F. Vewinger, and M. Weitz, *Nature* **468**, 545 (2010).
 - [20] V. May and O. Kuhn, *Charge and Energy Transfer Dynamics in Molecular Systems*, 3rd ed. (John Wiley & Sons, Ltd, 2011).
 - [21] M. Reitz, C. Sommer, B. Gurlek, V. Sandoghdar, D. Martin-Cano, and C. Genes, *Phys. Rev. Research* **2**, 033270 (2020).
 - [22] M. Reitz and C. Genes, *J. Chem. Phys.* **153**, 234305 (2020).
 - [23] Y. Zhang, J. Aizpurua, and R. Esteban, *ACS Photonics* **7**, 1676 (2020).
 - [24] J. Johansson, P. Nation, and F. Nori, *Comput. Phys. Commun.* **184**, 1234 (2013).
 - [25] R. Sawant, O. Dulieu, and S. A. Rangwala, *Phys. Rev. A* **97**, 063405 (2018).
 - [26] T. Schwartz, J. A. Hutchison, C. Genet, and T. W. Ebbesen, *Phys. Rev. Lett.* **106**, 196405 (2011).
 - [27] W. H. Miller, N. C. Handy, and J. E. Adams, *J. Chem. Phys.* **72**, 99 (1980).
 - [28] J. Calvo, D. Zueco, and L. Martin-Moreno, *Nanophotonics* **9**, 277 (2020).
 - [29] R. S. Sánchez-Carrera, M. C. R. Delgado, C. C. Ferrón, R. M. Osuna, V. Hernández, J. T. L. Navarrete, and A. Aspuru-Guzik, *Organic Electronics* **11**, 1701 (2010).
 - [30] F. Herrera and F. C. Spano, *Phys. Rev. A* **95**, 053867 (2017).
 - [31] F. Herrera and F. C. Spano, *ACS Photonics* **5**, 65 (2018).
 - [32] J. A. Ćwik, P. Kirton, S. De Liberato, and J. Keeling, *Phys. Rev. A* **93**, 033840 (2016).
 - [33] K. B. Arnardottir, A. J. Moilanen, A. Strashko, P. Törmä, and J. Keeling, *Phys. Rev. Lett.* **125**, 233603 (2020).
 - [34] P. Z. Crispin Gardiner, *Quantum noise: A Handbook of Markovian and Non-Markovian Quantum Stochastic Methods with Applications to Quantum Optics*, 2nd ed., Springer series in synergetics (Springer-Verlag, Berlin Heidelberg, 2004).
 - [35] A. Nitzan, S. Mukamel, and J. Jortner, *J. Chem. Phys.* **63**, 200

- (1975).
- [36] M. Radonjić, W. Kopylov, A. Balaž, and A. Pelster, *New J. Phys.* **20**, 055014 (2018).
 - [37] J.-H. Li, J.-B. Liu, A.-X. Chen, and C.-C. Qi, *Phys. Rev. A* **74**, 033816 (2006).
 - [38] D. Plankensteiner, C. Sommer, M. Reitz, H. Ritsch, and C. Genes, *Phys. Rev. A* **99**, 043843 (2019).
 - [39] F. Bernardot, P. Nussenzveig, M. Brune, J. M. Raimond, and S. Haroche, *EPL* **17**, 33 (1992).
 - [40] G. Khitrova, H. M. Gibbs, M. Kira, S. W. Koch, and A. Scherer, *Nat. Phys.* **2**, 81 (2006).
 - [41] D. Wellnitz, S. Schütz, S. Whitlock, J. Schachenmayer, and G. Pupillo, *Phys. Rev. Lett.* **125**, 193201 (2020).
 - [42] J. Galego, C. Climent, F. J. Garcia-Vidal, and J. Feist, *Phys. Rev. X* **9**, 021057 (2019).
 - [43] H. J. Carmichael, *Statistical Methods in Quantum Optics 1: Master Equations and Fokker-Planck Equations*, Theoretical and Mathematical Physics (Springer-Verlag, Berlin Heidelberg, 1999).
 - [44] M. Sauer, J. Hofkens, and J. Enderlein, *Handbook of Fluorescence Spectroscopy and Imaging: From Single Molecules to Ensembles* (Wiley-VCH Verlag GmbH & Co. KGaA, Weinheim, Germany, 2011).